Journal Pre-proof

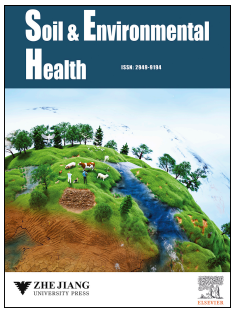

Stabilizing organic matter and reducing methane emissions in composting with biochar to strengthen the role of compost in soil health

Keiji Jindo, Tomonori Sonoki, Miguel A. Sánchez-Monedero

PII: S2949-9194(25)00037-8

DOI: https://doi.org/10.1016/j.seh.2025.100164

Reference: SEH 100164

To appear in: *Soil & Environmental Health*

Received Date: 24 February 2025

Revised Date: 26 June 2025

Accepted Date: 26 June 2025

Please cite this article as: Jindo, K., Sonoki, T., Sánchez-Monedero, M.A., Stabilizing organic matter and reducing methane emissions in composting with biochar to strengthen the role of compost in soil health, *Soil & Environmental Health*, https://doi.org/10.1016/j.seh.2025.100164.

Title: Stabilizing organic matter and reducing methane emissions in composting with biochar to strengthen the role of compost in soil health

Authors: Keiji Jindo[a]*, Tomonori Sonoki[b], Miguel A. Sánchez-Monedero[c]

[a]Agrosystems Research, Wageningen University & Research, P.O. Box 16, 6700 AA, Wageningen, the Netherlands. keiji.jindo@wur.nl

[b]Faculty of Agriculture and Life Science, Hirosaki University, Hirosaki, Aomori, 036-8561, Japan. sonoki@hirosaki-u.ac.jp.

[c]Department of Soil and Water Conservation and Organic Waste Management, CEBAS-CSIC, Campus Universitario de Espinardo, Murcia, Spain. monedero@cebas.csic.es

*Corresponding author: Keiji Jindo (keiji.jindo@wur.nl); Tel.: + 31 639072812

11

12 **Graphical Abstract**

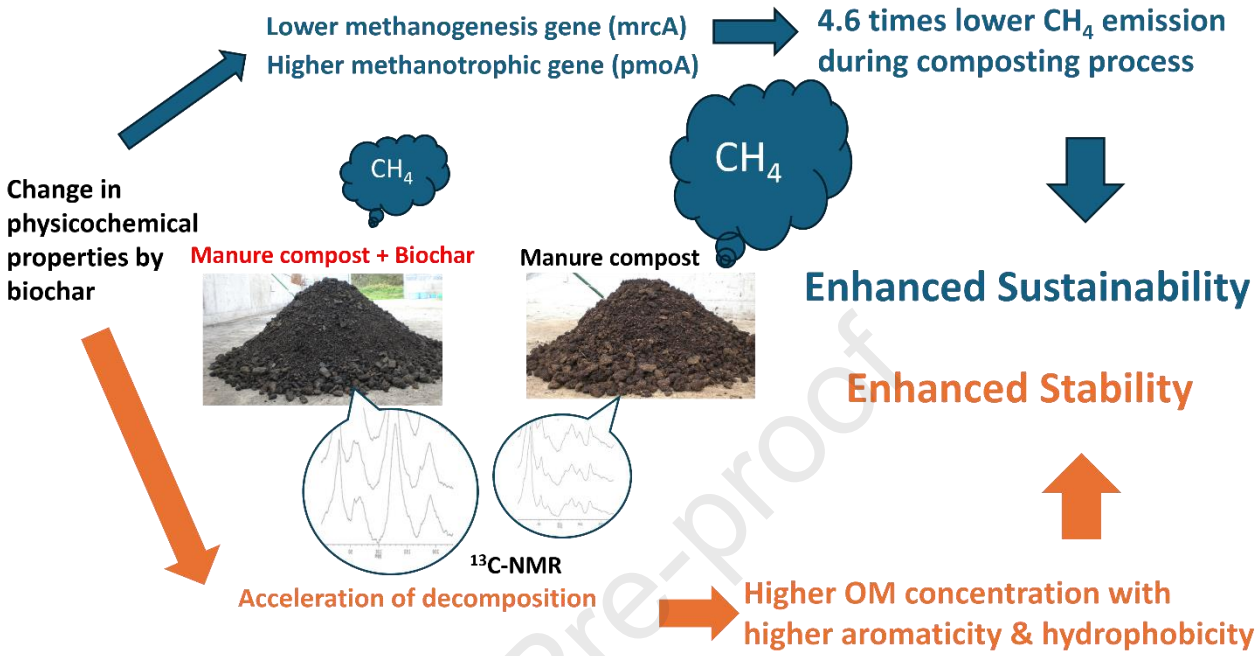

13

14

15

16 **Highlights**

17 • Biochar reduced methane emission 4.6-fold in poultry and 3.7-fold in cattle composts.

18 • Lignin degradation and stability were enhanced with biochar amendment.

19 • Biochar improved compost quality and carbon transformation for soil health.

Abstract: Biochar is a promising additive for enhancing composting efficiency and long-term compost quality. This study investigated its effects on greenhouse gas emissions and organic matter stabilization during the composting of poultry (PM) and cattle manure (CM). Biochar addition significantly reduced methane emissions during the thermophilic phase—by 4.6-fold in PM amended with biochar and 3.7-fold in CM amended with biochar compared to PM and CM without biochar amendment, respectively—indicating improved aeration and microbial activity, as supported by higher CO_2 emissions. A novel aspect of this study is the focus on lignin, a recalcitrant carbon fraction. Biochar-amended composts showed 1.5-fold greater lignin degradation (29.0% in PM+B and 10.8% in CM+B) than controls, along with enhanced lignin stability, as evidenced by Nuclear Magnetic Resonance (NMR) spectroscopy and thermal analysis. We assessed labile carbon fractions (e.g., water-soluble carbon, carbohydrates), ATP, and enzymes involved in carbon and nutrient cycling. PM and CM retained more labile carbon through the final stage, showing higher ATP, dehydrogenase, and β-glucosidase than their biochar-treated counterparts. Redundancy analysis (RDA) indicated that microbial communities and structural traits influenced gas emissions during the thermophilic stage and compost stabilization at the final stage. CH_4 emissions were associated with *mcrA*, fungi, and total nitrogen (TN), while CO_2 correlated with bulk density and Gram-negative bacteria. In the final stage, maturity indices were linked with microbial and physicochemical variables, underscoring their combined role in compost stabilization. Biochar amendment enhanced compost quality by reducing CH_4 emission and promoting selective carbon transformation, particularly lignin. These findings support biochar-composting as a strategy for producing composts with improved agronomic and environmental value.

Keywords: Lignin; Enzymatic Activities; Humification; Poultry manure; Cattle manure; ^{13}C-NMR; Methanogens; C cycle.

List of Abbreviations

Full name	Abbreviation
Bulk density	BD
Carbon dioxide	CO_2
Carbon-13 Nuclear Magnetic Resonance	^{13}C NMR
Cattle manure	CM
Cattle manure with biochar	CM+B
Fulvic acid	FA
Humic acid	HA
Humification index	HI
Methane	CH_4
Particulate methane monooxygenase gene (*pmoA*)	*pmoA*
Methyl-coenzyme M reductase	*mcrA*
Organic matter	OM
Phospholipid-derived fatty acids	PLFA
Polymerization degree	PZ
Poultry manure	PM
Poultry manure with biochar	PM+B
Redundancy analysis	RDA
Thermogravimetric analysis	TGA
Total nitrogen	TN
Water-soluble carbon: Organic nitrogen ratio	Cw/N_org

Introduction

Maintaining soil health is paramount in climate change, as healthy soil ecosystems play a pivotal role in carbon sequestration, thereby mitigating greenhouse gas emissions and the consequences of a changing climate. Compost offers multiple benefits to soil health by enriching organic matter, enhancing microbial activity, supplying essential nutrients, and improving physical properties (Cao et al., 2023). Moreover, the synergistic application of biochar and compost offers additional advantages, including reducing greenhouse gas emissions and promoting more stable carbon sequestration (Khan et al., 2023). Additionally, the increased organic matter (OM) content resulting from biochar addition to composting or after soil amendment could trigger a negative priming effect that reduces organic carbon (OC) mineralization (Wang et al., 2016; Khan et al., 2023).

Proper aeration and pile structure are essential for optimizing the composting process and preventing anaerobic conditions, which can result in incomplete decomposition of organic matter and lower compost quality. Under anaerobic conditions, methanogenic archaea become active, producing methane (CH_4) by reducing carbon compounds such as CO_2 and acetate due to the lack of oxygen (Fang et al., 2022; Yu et al., 2023; Zhai et al., 2025). One key advantage of incorporating biochar into composting is its high porosity, facilitating improved aeration within composting piles. The use of biochar as a bulking agent creates air spaces within the compost pile, promoting favorable conditions for microorganisms involved in organic matter degradation, stabilization, nutrient cycling and mitigation of CH_4 emission (Sanchez-Monedero et al., 2018).

Adding biochar enhances microbial activity, enabling even the more recalcitrant lignocellulosic components of organic material to break down more rapidly. This becomes especially important when combining raw materials with poor physical properties for composting. Moreover, previous research (Jindo et al., 2012) has shown that incorporating biochar reduces the bulk density of the composting pile, indicating increased porosity and improved airflow within the pile.

Biochar also offers prolonged stability compared to conventional materials such as woodchips. Although previous studies assessed its stability characteristics through thermogravimetry (Jindo et al., 2014), the extent of degradation of lignin, considered a recalcitrant carbon with aromatic structure during the composting process, remains relatively unexplored (Yu et al., 2019). Since a more recalcitrant and stable carbon plays a key role in soil health, it is worthwhile to investigate the longevity of the lignin carbon content of the organic materials from compost before amending to the soil. Although a number of studies report on the acceleration of the degradation of organic matter during composting by biochar addition (Pivato et al., 2023; Wang et al., 2023), there is little known about the relationship between the lignin degradation and biochar in the compost. A novelty of this study is the focus on lignin, a relatively recalcitrant carbon fraction.

Recently, various approaches have been developed to enhance lignin degradation in composted organic waste, including the inoculation of lignocellulose-degrading microorganisms and the use of activated persulfate (Ji et al., 2023; Wang et al., 2021; Yu et al., 2023; Zhai et al., 2025). However, there is growing concern that such microbial inoculation may accelerate the metabolism of organic matter, leading to excessive CO_2 release. This could deplete oxygen levels, create anaerobic conditions, and consequently promote CH_4 emissions during composting (Yu et al., 2023). Our study aims to assess if biochar addition is a strong approach for lignin degradation and mitigation of CH_4.

Building upon our previous works (Jindo et al., 2016; Jindo et al., 2012; Sonoki et al., 2013), which focused on various aspects of carbon cycling in biochar-enriched composts, including organic matter degradation, humification, and CH_4 emissions, this study delves deeper into the carbon stability in biochar-enhanced composts. Sonoki et al. (2013) revealed that the proportion of *mcrA* was decreased with biochar addition, whereas *pmoA* was increased during the early stages of composting. This is important since mitigating CH_4 emissions during composting promotes more efficient aerobic composting, leading to a final product with higher organic matter stability and nutrient availability. While other additive products are promoted, such as membrane for mitigation of CH_4 (Fang et al., 2022; Yu et al., 2023; Zhai et al., 2025), biochar does not only mitigate GHG reduction but also

provides other multiple benefits for final products, such as enhancement of physicochemical properties (e.g. water retention, bulk density, carbon storage). When added to soil, this improved compost enhances long-term soil structure, microbial activity, and carbon sequestration, benefiting soil health over time (Khan et al., 2023; Wang et al., 2016; Yuan et al., 2017).

This study aims to comprehensively examine the effects of biochar addition on the quality and stability of organic matter in mature compost to produce a high-quality amendment that supports long-term soil health. First, we assessed the effect of biochar addition on methane emissions as an indirect indicator of composting efficiency. Then, we examined how biochar addition influences the stabilization of recalcitrant carbon, focusing on changes in lignin content throughout the composting process. We hypothesize that hardwood biochar produced at 550 °C may influence lignin decomposition during composting. Additionally, we examined whether biochar itself partially degrades, with oxidized fractions potentially integrating into the lignin pool and contributing to humic substance formation. These processes may enhance humification, as seen in our previous work (Jindo et al., 2015) and result in a more stable compost end product. Later, we assessed other more labile carbon fractions (e.g. soluble organic C and carbohydrate) and microbial activity indicators linked to nutrient cycles. Lastly, redundancy analysis (RDA) was employed to provide a comprehensive understanding of the effects of biochar addition in the composting process, focusing on CH_4 emission reduction and the stability of the composted material.

Material and Methods

Biochar material

Hardwood biochar was generated from *Quercus serrata*, a broad-leaved tree, using a traditional Japanese kiln. The biochar underwent a slow pyrolysis process at 550 °C under atmospheric pressure. To assess the biochar's properties, it was ground and sieved until its diameter measured less than 0.5 mm. The resulting biochar exhibited the following key attributes: a pH level of 7.23, a carbon content

of 791 g kg^{-1}, an oxygen content of 91.5 g kg^{-1}, a nitrogen content of 37.6 g kg^{-1}, a hydrogen content of 18.9 g kg^{-1}, a potassium content of 14.1 g kg^{-1}, and a phosphorus content of 2.3 g kg^{-1}. The biochar's physical characteristics included an extensive surface area measuring 255 m^2. The absorption capacity for methylene blue, measured for microporosity, is 8.3 mg $g^{-1,}$ while the iodine adsorption capacity, considered as a mesoporosity of biochar material, is 100 mg g^{-1}. While the Cross-polarization magic angle spinning (CPMAS) ^{13}C nuclear magnetic resonance (NMR) was applied to identify different carbon groups in the biochar (Supplemental Information Fig. 1.), thermogravimetric analysis (TGA) was used to assess the thermal stability of the biochar (Supplemental Information Fig. 2). In NMR, the dominant peak around 130 ppm indicates a high abundance of aromatic carbon structures, while smaller peaks near 170–190 ppm suggest the presence of carboxylic and carbonyl group. A faint signal below 60 ppm may reflect residual aliphatic or O-alkyl carbons, representing relatively more degradable organic fractions. The TGA profile of hardwood biochar produced at 550 °C showed minimal weight loss (1.7%) below 300 °C due to moisture and light volatiles, followed by a major decomposition event between 300–550 °C (89.4% weight loss) attributed to the oxidation of amorphous and semi-aromatic carbon structures, with a peak heat flow observed at ~450 °C. The residual mass (7.8%) above 550 °C likely corresponds to thermally stable inorganic ash and condensed aromatic carbon.

Composting was conducted at Hirosaki University's Kanagi experimental farm throughout the summer and autumn seasons. Two mixtures, each comprising CM and PM (totalling 100.9 kg), were formulated by combining apple pomace (76.8 kg), rice straw (9.7 kg), and rice bran (12.7 kg). An additional 20 kg of biochar was introduced into each mixture (CM+B and PM+B). Control treatments were also prepared, consisting of composting mixtures without biochar addition (CM and PM). No microbial inoculums were applied to support the composting. The organic waste mixtures were shaped into cone-shaped windrows, each with a volume of 0.7065 m^3. To promote aeration and ensure uniformity within the organic materials, the mixtures were turned twice weekly during the initial week and once weekly from the second week onwards. Temperature measurements for each pile were

continuously recorded using a thermo-recorder from T&D Co., Ltd., Nagano, Japan (Supplemental Information Fig. 3). All compost piles exhibited a typical temperature profile, rising from an initial 31–33 °C to thermophilic conditions (>55 °C) within the first few days and maintaining this phase for approximately 20–25 days. A gradual temperature decline toward ambient levels followed this. Biochar addition led to a more rapid rise in temperature (see Supplementary Information). The moisture content of the material was maintained at approximately 60% by adding water. The composting process spanned approximately three months for each pile. Multiple subsamples were collected from different locations within each composting pile and then thoroughly mixed to create a homogeneous composite sample for analysis. Representative samples of the organic material were collected at several distinct stages of the composting process: From the initial mixture during the thermophilic phase, during the 1st week (T1) and the 2nd week of composting (T2), During the mid-and end-stage of the thermophilic phase after the 3rd and 4th weeks (T3 and T4, respectively); During mesophilic stage after six weeks (T5); and The end of mature stage after 12 weeks (T6, respectively). These samples were composited from randomly selected subsamples taken from five different locations within the piles, spanning from top to bottom. Subsequently, they were air-dried and ground to a particle size of 0.5 mm to ensure material homogeneity.

Emission of methane (CH_4) and carbon dioxide (CO_2)

CH_4 flux measurements were conducted at 7-day intervals, commencing on day 21, using the static chamber method with a 13-litre polycarbonate chamber equipped with a gas sampling port. A 250 mL gas sample was extracted into a Tedlar® bag at three-time points: 0, 10, and 20 minutes after closing the chamber. CH_4 and CO_2 content were determined using gas chromatography (Agilent Inc., CA, USA, 7890A valve system) with two types of columns: Pora pack Q (Agilent Inc.) and MS-5A (Agilent Inc.). The gases were separated in the columns and guided to a flame ionization detector (FID), via a nickel catalyst in which CO_2 was reduced to CH_4, to quantify CH_4 and CO_2. The column oven temperature was maintained at 50°C, and Argon (Ar) was used as the carrier gas with a flow rate

of 3.5 mL/min. The FID was operated at temperature of 250°C. Samples were collected at three time points, although one was excluded due to unsuccessful measurement.

Easy-degradable carbon group

Total dissolved organic carbon was determined in a 1:10 extract with a liquid sample TOC analyzer (Shimadzu 5050A, Kyoto, Japan). Additionally, water-soluble carbohydrates were quantified using the anthrone method (Brink et al., 1960) in the same extract, and water-soluble phenols were measured using a modified version of the Folin method (Kuwatsuka and Shindo, 1973). Those measurements were taken three times.

Recalcitrant carbon assessment

Lignin was determined by the American National Standards methodology (ANSI/ASTM, 1977). The Klason Lignin method is the most commonly used technique for lignin analysis. In this method, Klason lignin refers to the residue obtained after the total acid hydrolysis of the carbohydrate portion of wood. Treatment with sulfuric acid hydrolyzes polysaccharides into water-soluble sugars, leaving lignin as an insoluble residue. The process begins by extracting lignocellulose with a mixture of benzene and ethanol. Then, 72% concentrated sulfuric acid is added, and the reaction is carried out at 30°C for 4 hours. Afterwards, the sulfuric acid is diluted to 3%, and the mixture is refluxed for an additional 2 hours. Finally, the insoluble residue is collected and weighed as lignin. The lignin content measurement was duplicated. The losses of lignin were calculated according to the equation originally used for the losses of the whole OM (Paredes et al., 2000): Lignin-loss (%) = 100-100 [(X1Lignin2) / (X2Lignin1)]; where X1 and X2 are the initial and final ash concentrations, and lignin1 and lignin2 are the initial and final lignin concentrations. To identify the different carbon groups, ^{13}C NMR spectra were used. ^{13}C-NMR spectra were acquired on the solid samples with a Varian 300 spectrometer (Varian Inc, CA, US) equipped with a 4-mm wide-bore MAS probe operating at a ^{13}C resonance

frequency of 75.47 MHz. The spectra were analyzed by dividing the chemical shift (ppm) resonance range into distinct intervals as follows: 0–46 ppm (encompassing alkyl C, predominantly CH_2 and CH_3 sp^3 carbons), 46–65 ppm (including methoxy and N alkyl C originating from OCH_3, and complex aliphatic carbons), 65–90 ppm (comprising O-alkyl C, such as alcohols and ethers), 90–108 ppm (corresponding to anomeric carbons found in carbohydrate-like structures), 108–160 ppm (representing aromatic carbons), 160–185 ppm (covering carboxyl, amides, and esters), and 185–225 ppm (encompassing carbonyls). The aromatic index values were determined following the methods outlined by other works (Palanivell et al., 2013; Wang et al., 2014), using the formula: aromaticity index (AI) = (aromatic C) / (alkyl C + N-alkyl C + O-alkyl C + aromatic C) × 100. Similarly, the hydrophobicity index was calculated based on previous studies (Canellas et al., 2012; Spaccini et al., 2002) as Hydrophobic C/Hydrophilic C = (alkyl C + aromatic C) / (N-alkyl C + O-alkyl C + anomeric C + carboxyl, amides, ester).

Biochemical and enzymatic assessment

Adenosine triphosphate (ATP) was extracted according to the procedure outlined by Webster et al. (1984) and quantified using the luciferin-luciferase assay in a luminometer (Optocom 1, MM Instruments, Inc.). Dehydrogenase activity was determined by reducing 2-p-iodophenyl-3-p-nitrophenyl-5-phenyltetrazolium chloride (INT) to iodonitrophenyl-formazan (INTF), and its absorbance was measured at 490 nm using a spectrophotometer, following the method in previous study (Wei et al., 2022). Microbial biomass carbon was assessed via the fumigation-extraction method. Organic C was extracted using K_2SO_4, and the carbon content in the K_2SO_4 compost extracts was determined using a TOC analyzer (Shimadzu TOC-5050A). β-glucosidase activity was determined by the colorimetric estimation of p-nitrophenol (PNP) formed during the hydrolysis of p-nitrophenyl-β-d-glucopyranoside (PNG), following the method described by Eivazi and Tabatabai, 1988. The activities of alkaline phosphatases were measured at 37 °C using p-nitrophenyl phosphate

(PNPP; Sigma N4645) as a substrate at pH 11 and expressed as μg PNP h^{-1} g^{-1} dry compost (Li et al., 2021). All those measurements were taken three times per treatment.

Statistical analysis

For statistical analysis of the emission of CH_4 and CO_2, Welch's t-test and Cohen's d effect size were conducted. All other results are reported as means with one-way ANOVA followed by Tukey's post-hoc test (HSD, honestly significant difference at the 95% confidence interval). The statistical analyses were conducted with the R program (Rstudio 3.5.1 version, RStudio, Boston, MA, USA). The standard deviation is expressed as the bar. Redundancy Analysis (RDA) was conducted separately for the early and final stages of composting to understand treatment effects by using those parameters of the composting process. The objective for RDA at the early stage was to explore possible drivers of CH_4 variability, which only occurs during, while that of the final stage was to find possible drivers of the stability of compost product. 3 replicate data was used for RDA. K-Nearest Neighbors (KNN) imputation was conducted to find missing values for the variables that have two replicate data. KNN was based on Euclidean distance across all numeric variables. The R package VIM was used for KNN imputation. Scaling was done prior to RDA. The variables used for RDA included physicochemical properties, carbon fractions, biomass indicators, enzymatic activities, and the relative abundances of phospholipid-derived fatty acids (PLFAs). Microbial community data were sourced from our previous study (Jindo et al., 2012; Sonoki et al., 2013), and chemical properties from Jindo et al. (2016). Variable names and abbreviations are listed in the supplemental information. In the thermal stage, response variables were CH_4, CO_2, the methane monooxygenase gene (*pmoA*), the methyl coenzyme M reductase gene (*mcrA*), and their ratio (*pmoA*/*mcrA*). For the final stage, response variables were the polymerization index (PZ), humification index (HI), and the ratio of water-soluble carbon to organic nitrogen (Cw/Norg), which are established maturity indices (Swarnam et al., 2016). The following explanatory variables were included in both stages: total nitrogen (TN), total carbon

(TC), pH, organic matter (OM), bulk density (BD), Gram-positive bacteria (Gram_P), Gram-negative bacteria (Gram_N), their ratio (GramP_GramN), total bacteria, fungi, the fungi-to-bacteria ratio, saturated and monounsaturated fatty acids, water-soluble carbon (WSC), ATP, β-glucosidase, alkaline phosphatase, dehydrogenase, water-soluble polyphenols, and carbohydrates. The W2/W1 ratio of lignin was used in the thermal stage, while lignin content was used in the final stage.

Result and discussion

CH_4 emissions during composting

In this research, we proposed the idea that the porous quality of biochar promotes air circulation within the compost mixture, thus hindering the release of CH_4 during composting with charcoal. As anticipated, CH_4 emission rate was significantly reduced in the presence of biochar, as depicted in Fig. 1. After 20 days of composting initiation, the CH_4 emission rate in the biochar-absent mixture of poultry manure (PM) reached approximately 570 mg of CH_4 per day per square meter. Conversely, in poultry manure composting with biochar (PM+B), the CH_4 emission rate was approximately 120 mg of CH_4 per day per square meter. These results manifest that in treatment "PM+B", CH_4 emissions decreased by approximately 4.6 times compared to PM without biochar (123 vs 572 mg CH_4 kg^{-1} DM). Additionally, we observed a secondary phase of CH_4 emission around day 42 in composting, and this, too, was mitigated by the inclusion of biochar (Fig. 1).

Regarding cow manure composting (Fig. 1), in treatment "CM+B", CH_4 emissions were reduced by approximately 3.7 times compared to CM (8.4 vs. 31.5 mg CH_4 kg^{-1} DM). It is crucial to highlight that introducing biochar into the composting process substantially decreased CH_4 emissions by enhancing the aeration in the composting pile. Other studies (Jyoti et al., 2022) report that adding biochar facilitated CH_4 oxidation and reduced CH_4 production by microorganisms. In the case of biochar addition, the enhancement of aerobic conditions within the composting mixture, thanks to its porous structure and large surface area, played a pivotal role in the remarkable reduction of CH_4 emissions by

influencing microbial activities associated with CH_4 production and oxidation (Sonoki et al., 2013). Adding biochar functions as a structural matrix and its porous nature may enhance oxygen carriers' performance, potentially restricting methanogens' adaptability to the environment (Guo et al., 2021).

It should also be highlighted that the type of biochar with different physical properties (e.g. pore size and bulk density) changes the magnitude of the CH_4 reduction during the composting. It is reported (Zhou et al., 2022) that wood biochar reduced more CH_4 than corn cob biochar due to smaller pore structure.

The reduced CH_4 emission in the biochar-blended compost is associated with the improved quality of the end-product, such as increasing functional groups and CEC (Chen et al., 2017) as well as the efficiency of composting in terms of the cost of the operation due to a reduction in composting time span by enhancing organic matter decomposition with higher aeration (Xiao et al., 2017).

Carbon dioxide emissions during composting

A gradual decrease in the amount of CO_2 was observed from the initial stage to the end of the composting process (Figure 2). Regarding the impact of biochar addition, at day 21 of composting, although Welch's t-test suggested a higher CO_2 concentration in the composts with biochar (PM+B, mean = 149 ppm; CM+B, mean = 209 ppm) compared to compost without biochars (PM, mean = 123 ppm; CM, mean = 175 ppm), the result was not statistically significant ($p > 0.05$), likely due to the limited sample size (n = 2 per group). Nevertheless, the moderate effect size (Cohen's d = 0.8) indicates a potentially meaningful difference. Emissions in treatments "PM+B" and "CM+B" were significantly higher than in PM and CM ($p < 0.05$), with extremely large effect sizes (Cohen's d = 9.32 and 13.6, respectively), suggesting enhanced microbial activities or OM decomposition with biochar. Our result of reduced CH_4 and increased CO_2 emission during the thermophilic phase of composting with biochar aligns with previous report (Gu et al., 2025). These findings suggest that the physical changes in the compost pile induced by biochar—such as lower bulk density, higher porosity, and greater specific surface area—likely enhanced air circulation, thereby influencing microbial activity by

299 improving habitat conditions and metabolic processes involved in organic matter degradation.
300 Although the sample size was small (n = 2 per group), the observed differences were statistically
301 significant. However, further studies with larger sample sizes are necessary to verify these findings.

302

303 *Quantitative and qualitative changes in the lignin fraction during composting*

304 Generally, lignin degradation during composting occurs in two main phases: the thermophilic
305 phase at the beginning and the cooling phase at the end. The primary microbial groups responsible for
306 lignin breakdown differ between these phases. Actinomycetes dominate during the thermophilic stage,
307 while white-rot fungi are more active during the later cooling stage.

308 In the biochar-amended treatments (PM+B and CM+B), the proportion of organic matter,
309 excluding the lignin fraction, is smaller due to the added biochar content (Figure 3). Our results
310 indicate that lignin degradation was most pronounced during the thermophilic stage (from T1 to T4).
311 This can be attributed to the presence of heat-tolerant actinomycetes and fungi capable of surviving
312 above 50 °C. These microbes produce ligninolytic enzymes—such as lignin peroxidase, manganese
313 peroxidase, and laccase—that biochemically degrade lignin under high-temperature, aerobic
314 conditions.

315 Differences were also observed between the types of manure. In the PM and PM+B piles,
316 lignin degradation occurred gradually from T1 to T6. In contrast, cow manure (CM and CM+B)
317 showed a more rapid decrease in lignin content between T3 (day 14), when pile temperatures exceeded
318 64 °C, and T4 (day 28), when temperatures declined to around 45–50 °C.

319 Composts amended with biochar (treatments “PM+B” and “CM+B”) showed significantly
320 higher lignin degradation than those without biochar (Table 1). Specifically, 29.% and 10.8% of lignin
321 were degraded in treatments “PM+B” and “CM+B”, respectively—approximately 1.5 times greater

than in the non-biochar treatments (PM and CM). These findings are consistent with the results of another report (Ma et al., 2024).

It is well-documented that biochar enhances microbial activity during the initial stages of composting, leading to faster temperature increases and an extended thermophilic period (Zainudin et al., 2020). Consequently, CO_2 emissions tended to be higher in biochar-amended composts (Fig. 2). Notably, lignin is highly resistant to degradation under anaerobic conditions, as its key oxidative enzymes require oxygen to function. Therefore, lignin breakdown in composting is primarily driven by aerobic, heat-tolerant microorganisms such as *Streptomyces* and *Promicromonospora* (Oviedo-Ocaña et al., 2025; Yu et al., 2023). Studies have reported that the addition of biochar to composting piles of green waste and food waste can result in lignin loss ranging from 28% to 33%, accompanied by increased abundance of these lignin-degrading microbes (Oviedo-Ocaña et al., 2025).

One of the primary aims of analyzing the changes in the lignin fraction was to assess its transformation as an indicator of organic matter recalcitrance in mature compost. This study demonstrated an increase in lignin concentration by incorporating biochar but also revealed qualitative changes in the lignin composition during composting, as measured by TGA analysis and ^{13}C-NMR.

Thermogravimetry analysis (TGA) is the most used tool to obtain experimental kinetic data for lignocellulosic biomass pyrolysis. The result of TGA in Supplemental Fig. 2 represents the characteristic of the stability of the hardwood biochar in our study produced at 550 °C. This recalcitrant nature of hardwood biochar enhanced compost thermal stability from the initial stage, with significant differences observed ($P < 0.05$; Table 2). Based on the W_2/W_1 ratio, stability increased by 2.8-fold in treatment "PM + B" and 4.4-fold in treatment "CM + B" compared to controls. At the final stage, this effect was even more pronounced ($P < 0.01$; Table 2), with similar fold increases: 2.6-fold for treatment "PM + B" and 4.7-fold for treatment "CM + B". The ^{13}C NMR spectra analysis is a strong tool to monitor the presence of lignin during the composting process. The use of ^{13}C NMR spectra is considered a reliable technique for understanding the distribution and content of organic molecules in a wide range of solid

organic matrices (Spaccini and Piccolo, 2009).. The ^{13}C NMR spectra of the PM lignin samples were dominated by peaks around 30-40 ppm corresponding to an alkyl group (Fig. 3, Supplementary Information, Fig. 4, left). Throughout the composting process, other moderate peaks at the beginning of the composting process became sharpened, such as the peaks at 55 ppm (methoxyl carbon), 127-130 ppm and 147-150 ppm (aromatic carbons), and 170-175 ppm (carboxyl carbon). Incorporating biochar into PM+B led to a gradual reduction in the sharp peak at 30–40 ppm, associated with aliphatic carbon, during the composting process. This was accompanied by a marked increase in aromatic groups, reflected in the sharp peak at 125–130 ppm (Shi et al., 2019), corresponding to the p-hydroxyphenyl units of lignin—one of its three main components, along with guaiacyl and syringyl (Supplementary Information Fig. 4, right side).

In the ^{13}C NMR spectra of cow manure with and without biochar (CM+B v.s. CM) (Supplementary Information Fig. 5), the same peaks are observed, although the shape of those peaks is more moderate compared to the poultry manure. The minor gap between PM and CM is seen in that the small peak around 70 ppm, attributed to carbohydrate in lignin, gradually disappears in PM toward the end of the composting process, while this peak gradually appears in CM in the middle of the process.

These parameters are commonly used as indicators of organic matter stability based on the distribution of different carbon groups (Bekier et al., 2014). Statistically significant differences ($p < 0.05$) were observed in the aromaticity index, with higher values in the biochar-amended treatments (PM+B and CM+B) compared to the non-biochar piles (PM and CM) (Table 2). Although hydrophobicity increased with biochar addition, the difference was insignificant. These results support the role of biochar in enhancing the recalcitrant properties of lignin and its resistance to microbial degradation within the compost pile. Continuously, these indicators of recalcitrance remained higher in the biochar-treated composts (PM+B and CM+B) at the end of the composting process, as shown in Table 2.

Biochar degradation during composting

Biochar degradation, influenced by feedstock type and pyrolysis conditions (e.g., temperature), plays a significant role in composting dynamics and soil responses, such as the priming effect (Nguyen et al., 2010; Wang et al., 2016). The hardwood biochar used in this study, which was produced at 550 °C, is considered relatively recalcitrant. Nevertheless, a reduction in the visible black biochar fraction (Fig. 2) was observed by the second week (T2) in treatment "PM + B" and the third week (T3) in treatment "CM + B", corresponding to the thermophilic stage (≥50 °C). This reduction may reflect oxidative degradation, as previous studies have shown that carbon loss from biochar increases with higher temperatures and that more stable biochar can be more sensitive to temperature-induced decomposition than less stable forms (Nguyen et al., 2010). The faint signal below 60 ppm in the ^{13}C NMR spectrum of our hardwood biochar (Supplemental Fig. 1), attributed to aliphatic or O-alkyl carbons, likely represents labile fractions that contribute to the early-stage mass loss (0–300 °C) seen in TGA (Supplemental Fig. 2), due to volatilization of light compounds and moisture.

Total dissolved carbon, carbohydrate, and water-soluble polyphenol fractions.

During composting, the microbes feed on easily decomposed compounds such as carbohydrates and proteins. Some of these turn into humic substances, as reported previously for these composting mixtures by Jindo et al (2016), while others are used as energy sources to support microbial activities. Fig 4 represents the changes in the concentration of total dissolved carbon throughout the composting process, which comprises typical easily-degradable compounds. It is shown that higher DOC contents are seen in both non-biochar compost (PM and CM). Carbohydrate and water-soluble polyphenols followed a similar pattern as sub-groups of dissolved organic carbon. All those easily degradable compounds are reduced mainly at the thermal stage. During the thermal stage, heat-tolerant microorganisms actively metabolize organic matter, converting carbohydrates into CO_2. This heightened microbial respiration can deplete oxygen locally, promoting the formation of anaerobic microsites that favor methanogenic activity and enhance CH_4 emissions.(Guo et al., 2021).

Composts without biochar showed higher levels of these soluble fractions, aligning with total dissolved organic carbon results (Fig. 4). Similar results about lower water-soluble carbon in compost with biochar are found in previous study (Hagemann et al., 2018). There are several possible mechanisms of biochar addition in relation with the reduction of the content of dissolved organic carbon: 1) Biochar enhanced the organic matter decomposition including dissolved carbon which accelerate the stability of the composted material (Xiao et al., 2017); and 2) easily-degradable compounds such as carbohydrate is retained in composting pile but not instead of degradation by microbes, this would be remained in composting pile even after the composting process such as incorporation in humified carbon fractions (Jindo et al., 2016) or absorption by biochar (Liu et al., 2024). Other researchers (Guo et al., 2021; Yu et al., 2023) report that the bacteria play an important role in consuming more dissolved organic carbon, including amino acids and carbohydrates, after being promoted by biochar and contributing to polymerization of carbon into a more stable form such as humic substances. Regarding lignin degradation and water-soluble carbon, Gu et al. (2025) reported that biochar may suppress methanogenic activity by reducing the availability of water-soluble carbon and increasing oxygen levels. The porous structure and alkaline nature of biochar are believed to create favorable conditions for methanotrophs in composting piles, thereby enhancing their capability to oxidize CH_4 and reduce CH_4 emissions.

ATP and dehydrogenase activity.

Analyzing ATP levels is a means of evaluating microbial activity since ATP functions as an energy carrier within cells. It serves as an indicator of metabolic activity and the viability of microorganisms. ATP is a vital molecule serving as the primary energy carrier in cells, including microbial ones. Its presence can signal the extent of metabolic activity and the overall viability of microorganisms in specific environments, such as composting piles or soil (Horiuchi et al., 2003). Dehydrogenase activity offers insights into the broader spectrum of soil microbial activity

(Piotrowska-Długosz et al., 2022). An additional method for gauging microbial activity is through the measurement of dehydrogenase activity, which yields valuable insights into overall microbial functioning. This enzyme is considered as an indicator of composting stabilization (Nikaeen et al., 2015).

In our study, PM and CM exhibit higher ATP and dehydrogenase levels than composts containing biochar (Fig. 5). This difference is likely attributed to the lower concentration of easily-degradable compounds (Fig. 4). At week 6, the range of dehydrogenase activity in CM with biochar (CM+B) was the same as at the end of the composting period. This suggests that a higher volumetric ratio of bulking agents (e.g., biochar, pruning waste, and sawdust) may have enhanced aeration, accelerating the composting process by facilitating organic matter stabilization (Nikaeen et al., 2015).

These findings are consistent with Jindo et al. (2012) who observed in the same composting mixtures that the changes in the microbial community structure caused by biochar were mostly driven by the original organic wastes.

Extracellular enzyme activity

B-glucosidase and alkaline phosphatase are both extracellular enzymes related to the cycling of carbon and phosphorus. Fig. 6 illustrates the effect of the biochar addition on those enzymatic activities during the composting process. At the end of the composting process (12 weeks), composts without biochar (PM and CM) exhibited higher enzymatic activities than the same mixtures enriched with biochar, which is related to the difference in the amount of easy-degradable compounds such as carbohydrates (Table 2). Same as the dehydrogenase, alkaline phosphatase in the CM with biochar (CM+B) was also stabilized from the week 6 to the end of the composting process (week 12) (Fig. 6). The different behaviour of enzymatic activity between compost with/without biochar is observed in alkaline phosphatase. On the contrary to other enzymatic activities such as dehydrogenase and *B*-glucosidase, both composts with biochar (treatments “PM+B” and “CM+B”) have higher alkaline

phosphatase compared to those without biochar (PM and CM) which is aligned with another work (Duan et al., 2022). The underlying mechanisms may include: (1) biochar promotes microbial communities such as mesophilic bacteria and thermophilic fungi possessing *phoD*, which contributes to phosphorus degradation; (2) the higher pH in biochar-amended compost may inhibit specific phosphorus-solubilizing microorganisms; (3) elevated pH may create more favorable conditions for alkaline phosphatases, which have an optimal pH around 11; and (4) previous studies have reported that compost enriched with lignocellulosic materials tends to exhibit higher phosphatase activity, possibly as a compensatory mechanism, which results in lower levels of inorganic phosphorus (El Fels et al., 2024).

Key factors determining the composting processes - Redundancy analysis (RDA)

Redundancy analysis (RDA) was used to integrate physicochemical, microbial, and metabolic data, offering insights into key factors shaping the composting process. The following section illustrates variable relationships during the thermophilic stage about CH_4 and CO_2 emissions (Fig. 7) and during the final stage in relation to compost maturity and stability (Fig. 8)

Thermophilic composting stage

RDA was conducted to assess the relationships between greenhouse gas emissions and key physicochemical and microbial variables during the thermophilic composting stage. The first two axes (RDA1 and RDA2) explained 89.6% of the constrained variance (RDA1: 63.4%, RDA2: 26.2%). CH_4 emissions and the abundance of the methanogenesis gene (*mcrA*) aligned closely with RDA1, while carbon dioxide (CO_2) and the methanotrophic gene (*pmoA*) showed strong negative associations with both axes. Fungal abundance and total nitrogen (TN) exhibited high positive loadings on RDA1, indicating a strong link with CH_4 production. In contrast, variables such as BD, Gram-negative bacteria (Gram_N), and lipid biomarkers (monounsaturated and saturated PLFAs) were more aligned with RDA2, pointing to their role in aerobic respiration and CO_2 fluxes. The lower bulk density (BD),

likely influenced by biochar addition, suggests improved aeration, which may have suppressed CH_4 formation ($r = 0.64$). Notably, Gram-positive bacteria (Gram_P) and bulk density (BD) exhibited similar vector directions in the RDA space (Fig. 7), suggesting a potential association between them. Previous studies (Chandna et al., 2013; Fracchia et al., 2006) have reported a high prevalence of Gram-positive organisms, particularly *Firmicutes* and *Actinobacteria*, during the thermophilic phase, as these microbes are heat-tolerant and capable of degrading lignocellulosic compounds. Biochar may offer a protective, nutrient-rich microenvironment that favors the proliferation of such bacteria. Their increased abundance could contribute to structural modifications within the compost matrix, thereby influencing bulk density during the thermophilic stage.

Overall, the constrained ordination revealed distinct microbial and structural controls over CH_4 and CO_2 emissions during the thermal stage, with ventilation, nitrogen availability, and microbial composition emerging as key drivers.

Final composting stage

In the final composting stage, RDA was employed to examine how microbial and physicochemical variables relate to compost maturity indicators. The first two axes accounted for 95.0% of the total constrained variance (RDA1: 56.5%, RDA2: 38.5%). The humification index (HI) strongly aligned with RDA1, while the polymerization index (PZ) and HA/FA ratio showed a positive relationship with RDA2. Conversely, the carbon-to-organic nitrogen ratio in the water-soluble fraction (Cw/N_org) was negatively associated with both axes, particularly RDA2, suggesting it decreased as compost matured. Bulk density, total nitrogen (TN), and ammonium (NH_4^+) were the major contributors to RDA1, reflecting their central role in the stabilization process.

Meanwhile, microbial characteristics—such as Gram-positive bacteria, total bacterial abundance, and fungi—loaded more strongly on RDA2, indicating their involvement in the biochemical transformation of organic matter. These patterns suggest that both structural factors (e.g., BD) and microbial community traits jointly regulate the transition toward more stable humified

compost. Despite the modest sample size, the ordination was well-structured and supported the relevance of these variables to the maturation dynamics.

Conclusion

This study demonstrates that incorporating biochar into composting provides dual benefits: it significantly lowers CH_4 emissions—by 4.6-fold in treatment "PM+B" and 3.7-fold in treatment "CM+B"—thereby reducing environmental impact, and it promotes the stabilization of organic matter. Notably, biochar enhanced the degradation of lignin, the most recalcitrant carbon fraction, by 29.0% in treatment "PM+B" and 10.8% in treatment "CM+B", approximately 1.5 times higher than in non-biochar treatments. Moreover, the remaining lignin became more chemically resistant, as indicated by increased stability indicators such as W_2/W_1 ratios with fold increases: 2.6-fold for treatment "PM + B" and 4.7-fold for treatment "CM + B", contributing to forming a more stable and mature compost product. In contrast, PM and CM contain other more labile carbon fractions till the final stage, consequently showing higher ATP, dehydrogenase and β-glucosidase than treatments "PM+B" and "CM+B". The RDA analyses revealed that microbial composition and structural properties significantly influenced gas emissions during the thermophilic stage and compost stabilization at the final stage. During the thermal phase, CH_4 emissions were associated with *mcrA* gene abundance, fungal biomass, and total nitrogen, while CO_2 emissions correlated with bulk density and Gram-negative bacteria. Biochar likely improved aeration (via reduced bulk density), suppressing CH_4 and promoting CO_2 release. In the final stage, compost maturity indicators (HI, PZ, HA/FA) were closely linked with both physicochemical traits (e.g., TN, NH_4^+, BD) and microbial variables (Gram-positive bacteria, total bacteria, fungi), indicating that compost stabilization was jointly governed by microbial activity and structural factors.

While our findings suggest that biochar-blended composts may offer more persistent organic matter and potential long-term benefits for soil health, this inference is based solely on compost characteristics. In addition to planning future soil incubation studies or field trials to evaluate the long-

term fate and impact of these composts after application, it is also important to integrate insights from previous soil studies to build upon existing knowledge.

Declarations

Availability of data and materials

Not applicable.

Competing interests

The authors declare that they have no competing interests.

Author Contributions

Conceptualization, K.J., and M.A.S.M.; methodology: M.A.M.S.; software: K.J.; validation: K.J. and M.A.M.S.; formal analysis: K.J., T.S., and M.A.M.S.; investigation K.J., T.S., and M.S.M.S. resources: T.S., and M.A.M.S.; data curation: K.J.; writing—original draft preparation: K.J.; writing—review and editing: K.J., T.S., and M.A.M.S.; visualization: K.J. and M.A.M.S.; supervision: K.J., T.S., and M.A.M.S.; project administration: T.S. and M.A.M.S.; funding acquisition: T.S. and M.A.M.S. All authors have read and agreed to the published version of the manuscript.

Funding

This research is financially supported by Agrosystems Research Group, Wageningen University & Research(Grant number 3710473400). This study is part of the project Ref: TED2021-131907B-I00, financed by the Spanish MCIN/AEI /10.13039/501100011033 and the European NextGenerationEU/PRTR funds.

Acknowledgement

We sincerely appreciate the financial support provided by the Japan Society for the Promotion of Science and the CSIC (Consejo Superior de Investigaciones Científicas) programs for this bilateral project. Miguel A Sanchez Monedero acknowledges funding from the Spanish Ministry of Science, Innovation and Universities (research project TED2021-131907B-I00). Keiji Jindo wishes to

550 acknowledge their financial support (3710473400). We appreciate Mr. Suto Koki for his technical
551 support.

552

553 Table 1. Lignin loss (%) in compost treatments with and without biochar from initial stage to
554 the end of the stage of composting process. PM: Poultry Manure; CM: Cow Manure; +B:
555 +Biochar.

.	N	Lignin loss (%)
PM+B	2	29.0 (0.1)
PM	2	18.6 (0.1)
P value		0.001
CM+B	2	17.0 (0.1)
CM	2	10.8 (0.1)
P value		0.004

556 Means were subjected to statistical analysis by the Welch´s-test. Value in parenthesis is
557 standard deviation

558

559

560

561

562

Table 2. Organic matter characteristics of the lignin fractions isolated at the initial and the end of the composting process. PM: Poultry Manure; CM: Cow Manure; +B: +Biochar. Aromaticity index and hydrophobicity are calculated from ^{13}C NMR spectra of the lignin. W_1/W_2 is calculated from the thermogravimentric analisis. Means were subjected to statistical analysis by the T-test. Value in parenthesis is standard deviation.

Phase	.Name	N	Aromaticity Index[*1]	Hydrophobicity[*2]	N	W_1/W_2[*3]
Initial	PM+B	2	45.7 (1.5)[*4]	2.54 (0.11)	2	0.251(0.022)
	PM	2	21.5 (2.9)	2.33 (0.85)	2	0.714 (0.110)
	P value		<0.05	n.s.		<0.05
	CM+B	2	42.6 (1.9)	2.71 (0.17)	2	0.219 (0.013)
	CM	2	26.2 (1.3)	2.13 (0.16)	2	0.963 (0.078)
	P value		<0.05	<0.1		<0.05
End	PM+B	1	45.4	2.54	2	0.247 (0.039)
	PM	2	27.6 (0.4)	2.33 (0.16)	2	0.652 (0.020)
	P value		-	-		< 0.01
	CM+B	1	39.8	2.63	2	0.141 (0.001)
	CM	1	29.7	2.00	2	0.6673(0.020)
	P value		-	-		< 0.01

[*1] Aromatic index = (aromatic C + phenolic C)/(alkyl C + N-alkyl C + O-alkyl C + aromatic C + phenolic C) $*$ 100.

[*2] Hydrophobic C (HB)/Hydrophilic C (HI) = (alkyl C + aromatic C + phenolic C)/(N-alkyl + O-alkyl C + anomeric C + carboxyl, amides, ester).

[*3] Ratio between the mass losses associated with the second (W2) and first (W1) exothermic reactions of thermal analysis.

Figure captions

Fig. 1. Methane (CH_4) generation rate during composting piles: poultry manure (PM); poultry manure with biochar (PM+B); cow manure (PM); cow manure with biochar (CM+B). Black lines represent manure composts without biochar, while red lines represent manure composts with biochars. The figure shows the mean value (n = 2), with error bars indicating the standard deviation of the samples. The asterisk indicates statistical significance ($p < 0.05$).

Fig. 2. CO_2 generation rate during composting piles: poultry manure (PM); poultry manure with biochar (PM+B); cow manure (PM); cow manure with biochar (CM+B). Black lines represent manure composts without biochar, while red lines represent manure composts with biochars. The figure shows the mean value (n = 2), with error bars indicating the standard deviation of the samples. The asterisk indicates statistical significance ($p < 0.05$).

Fig. 3. Distribution (%) of organic material over time.(Above) Poultry manure (PM, left) and poultry manure with biochar (PM+B, right); (Bottom) Cow manure (CM, left) and cow manure with biochar (CM+B, right). Color coding: Ash (gray), Lignin (brown), Organic matter excluding lignin (yellow), Degraded organic matter (blue), and Biochar (meshed black).Time points: T1 (1^{st} week); T2 (2^{nd} week); T3 (3^{rd} week); T4 (4^{th} week); T5 (6^{th} week); T6 (12^{th} week).

Fig. 4. Total dissolved carbon, carbohydrate, and water-soluble polyphenol in composting sampled from poultry manure (PM) and cow manure (CM) treated with biochar (PM+B and CM+B). The figure shows the mean value (n = 3), with error bars indicating the standard deviation of the samples. Asterisk mark represents the significant difference. *$p<0.05$.

Fig. 5. Adenosine 5-triphosphate (ATP) and dehydrogenase activity in composting sampled from poultry manure (PM) and cow manure (CM) treated with biochar (PM+B and CM+B). The figure shows the mean value (n = 3), with error bars indicating the standard deviation of the samples. Asterisk mark represents the significant difference. *$p<0.05$

Fig 6. β-glucosidase activity and alkaline phosphatase activity and in composting sampled from poultry manure (PM) and cow manure (CM) treated with biochar (PM+B and CM+B). The figure shows the mean value (n = 3), with error bars indicating the standard deviation of the samples. Asterisk mark represents the significant difference. *$p<0.05$.

Fig. 7. Correlation matrix between various indicators of organic matter stability and recalcitrance and key monitoring parameters of composting mixtures prepared from cattle manure (CM) and poultry manure (PM), with and without biochar. Data obtained from this study and from our previous our studies (Jindo et al 2012 & 2016). The list of the variables and its abbreviations are described in the supplemental material.

Fig 8. Biplot of principal component analysis with different variables Cow manure (CM, red dot); Cow manure with biochar (CM+B, green dot); poultry manure (PM, blue dot); poultry manure with biochar (PM+B, violet dot).

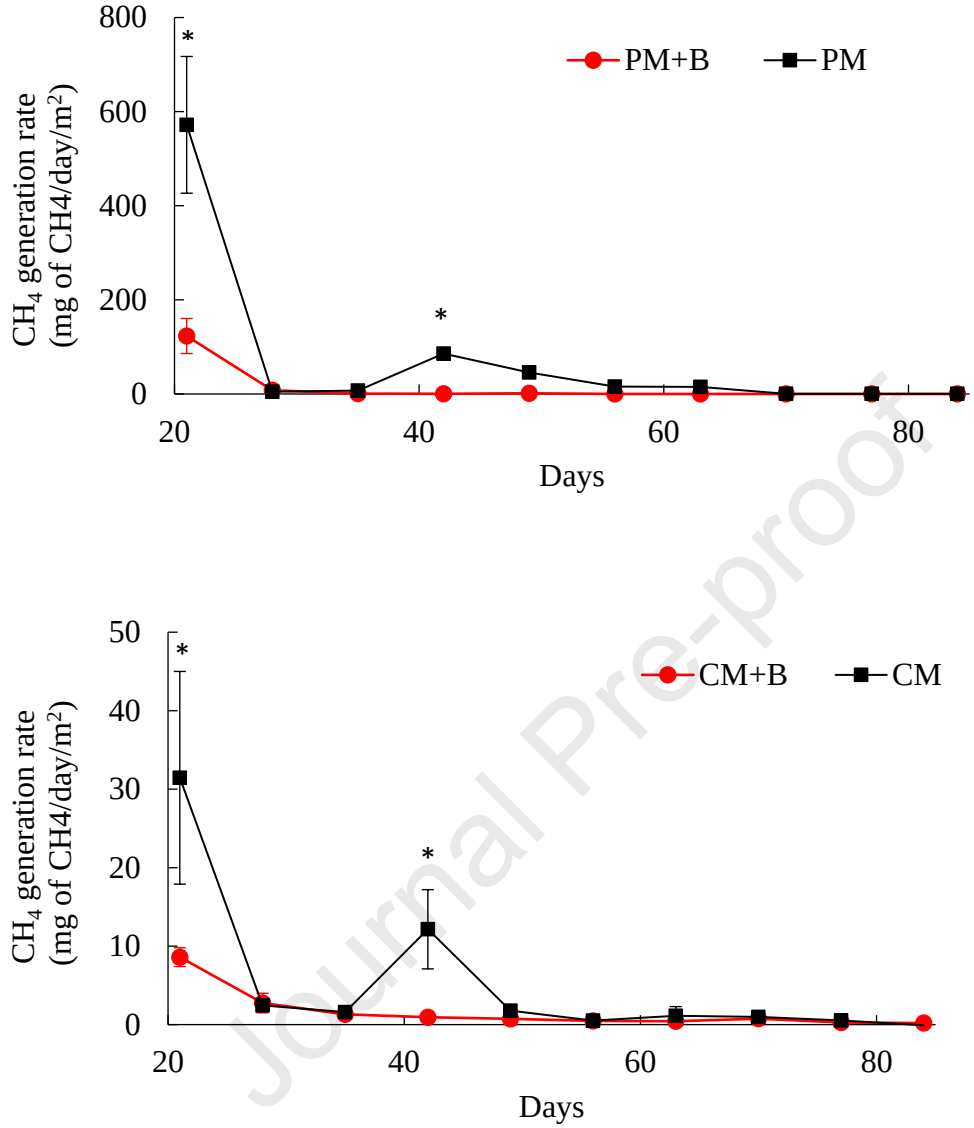

Fig. 1. Methane (CH_4) generation rate during composting piles: poultry manure (PM); poultry manure with biochar (PM+B); cow manure (PM); cow manure with biochar (CM+B). Black lines represent manure composts without biochar, while red lines represent manure composts with biochars. The figure shows the mean value (n = 2), with error bars indicating the standard deviation of the samples. The asterisk indicates statistical significance ($p < 0.05$).

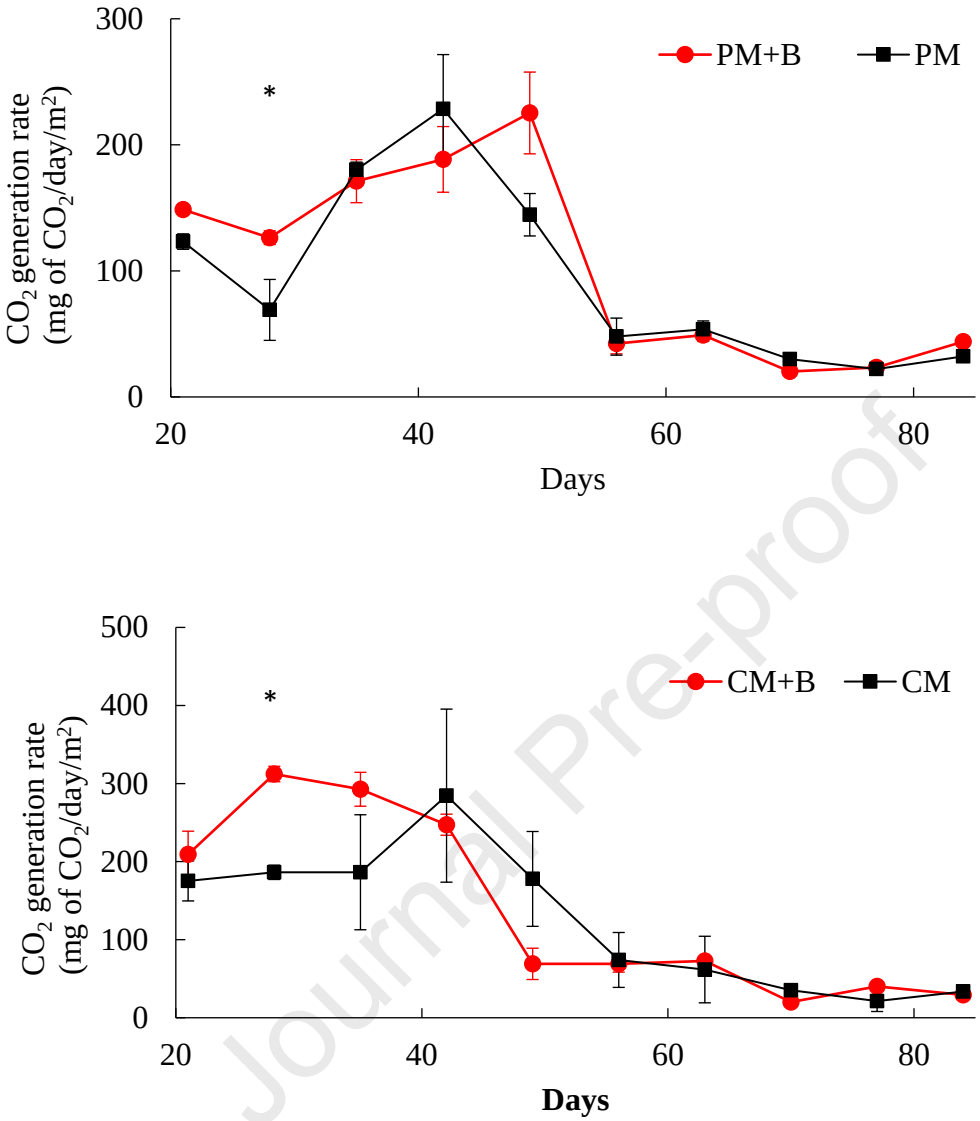

Fig. 2. CO_2 generation rate during composting piles: poultry manure (PM); poultry manure with biochar (PM+B); cow manure (PM); cow manure with biochar (CM+B). Black lines represent manure composts without biochar, while red lines represent manure composts with biochars. The figure shows the mean value (n = 2), with error bars indicating the standard deviation of the samples. The asterisk indicates statistical significance ($p < 0.05$).

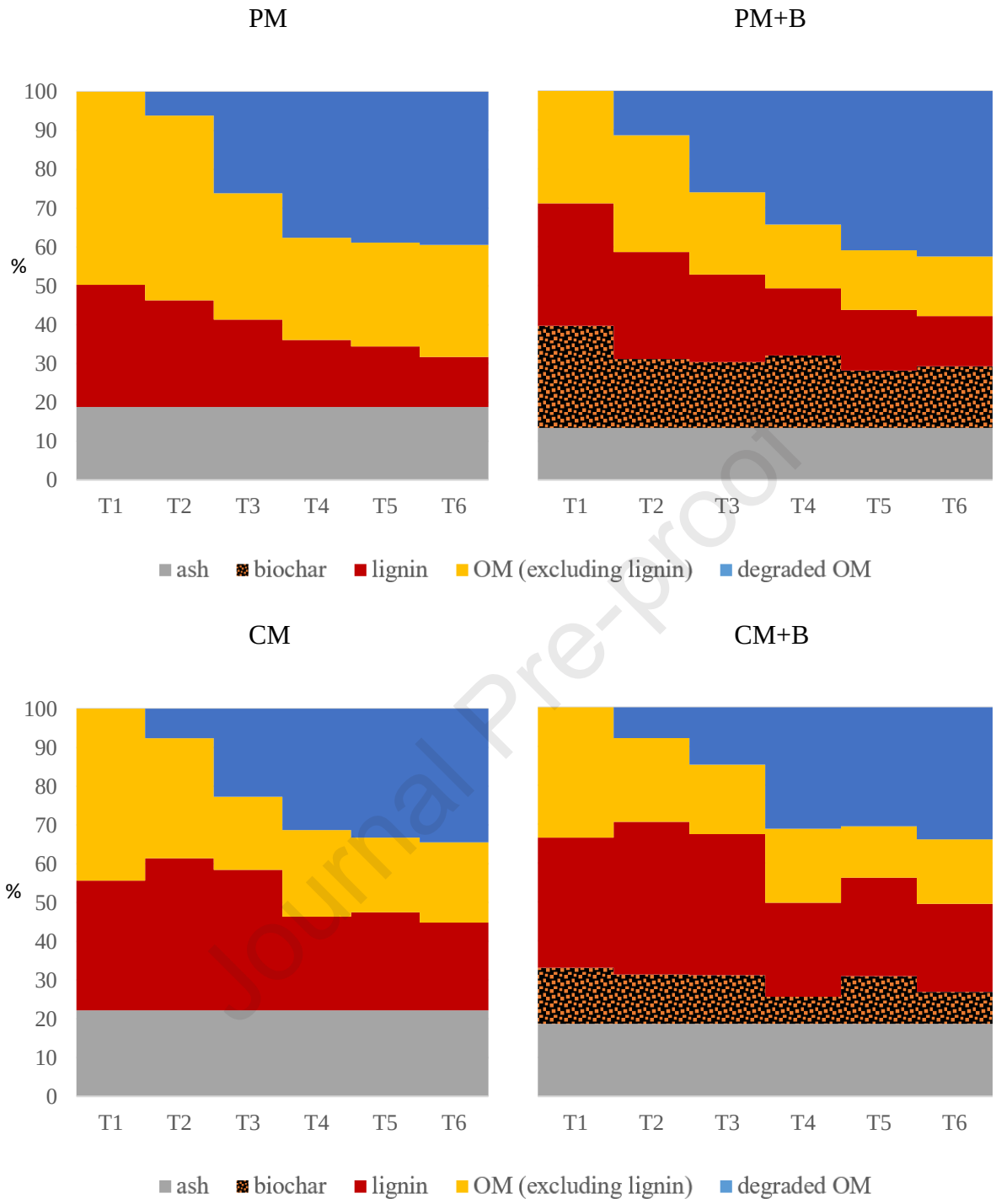

Fig. 3. Distribution (%) of organic material over time.(Above) Poultry manure (PM, left) and poultry manure with biochar (PM+B, right); (Bottom) Cow manure (CM, left) and cow manure with biochar (CM+B, right). Color coding: Ash (gray), Lignin (brown), Organic matter excluding lignin (yellow), Degraded organic matter (blue), and Biochar (meshed black).Time points: T1 (1st week); T2 (2nd week); T3 (3rd week); T4 (4th week); T5 (6th week); and T6 (12th week).

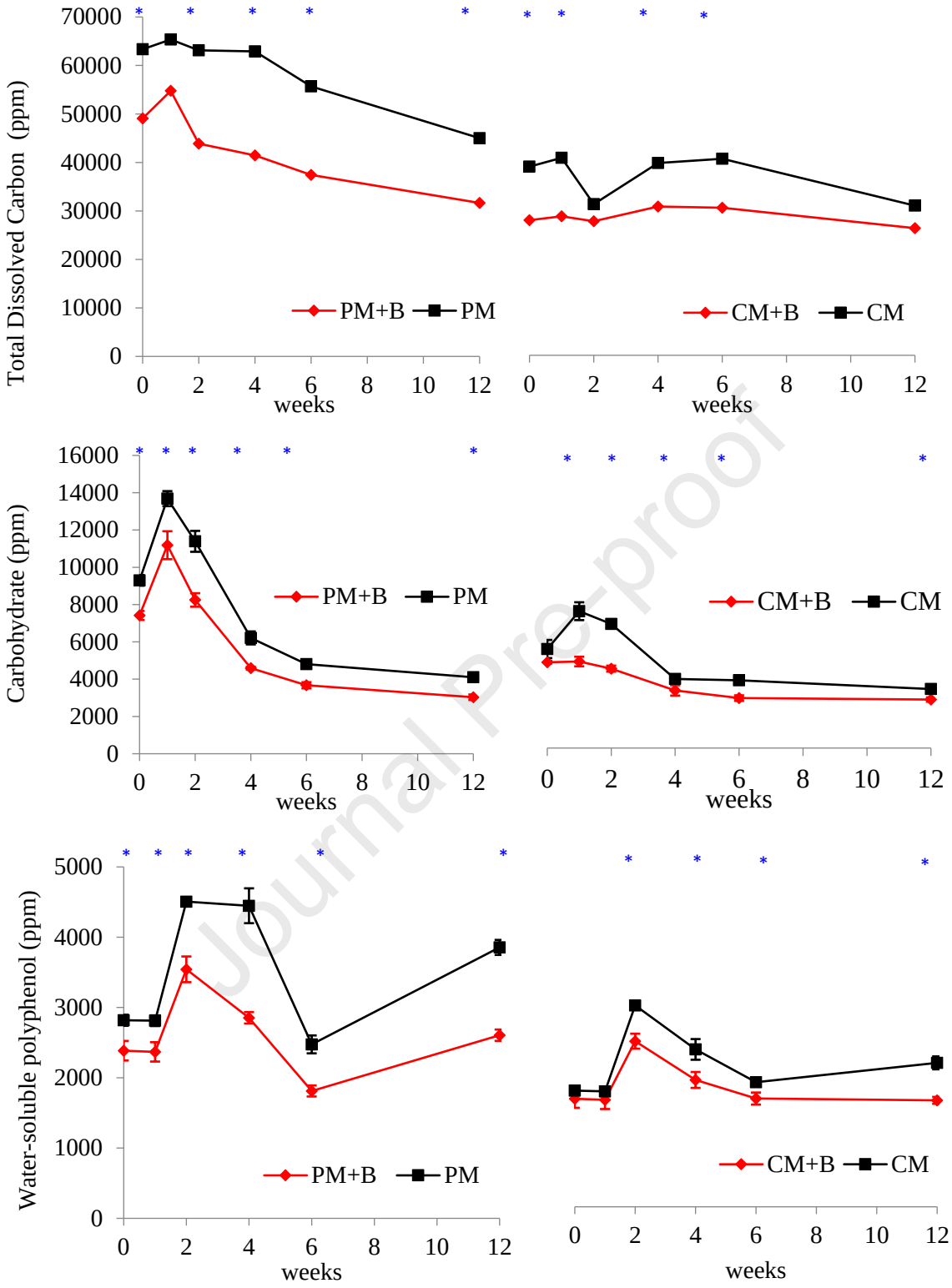

Fig. 4. Total dissolved carbon, carbohydrate, and water-soluble polyphenol in composting sampled from poultry manure (PM) and cow manure (CM) treated with biochar (PM+B and CM+B). The figure shows the mean value (n = 3), with error bars indicating the standard deviation of the samples. Asterisk mark represents the significant difference. *p<0.05.

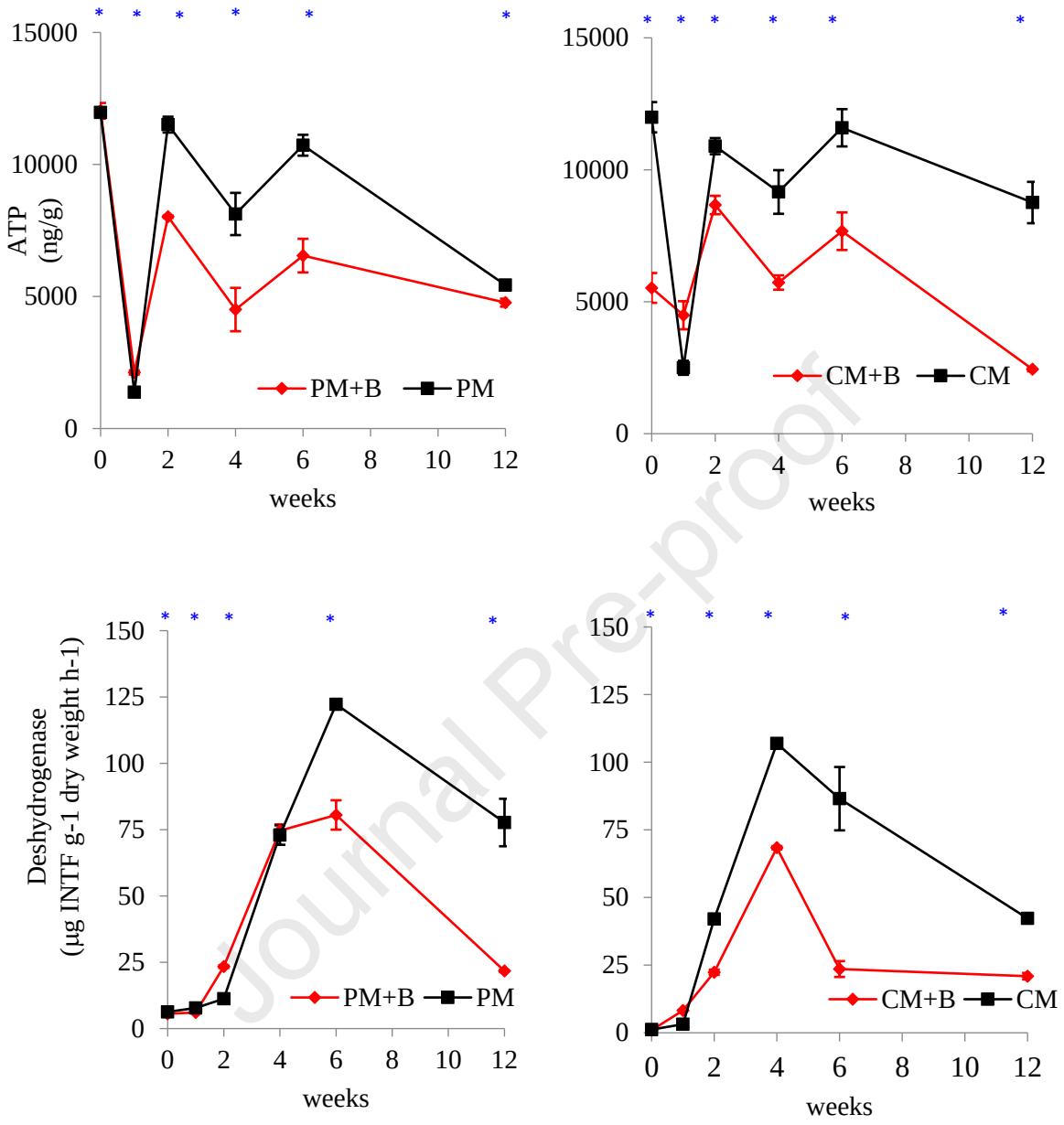

Fig. 5. Adenosine 5-triphosphate (ATP) and dehydrogenase activity in composting sampled from poultry manure (PM) and cow manure (CM) treated with biochar (PM+B and CM+B). The figure shows the mean value (n = 3), with error bars indicating the standard deviation of the samples. Asterisk mark represents the significant difference. *p<0.05.

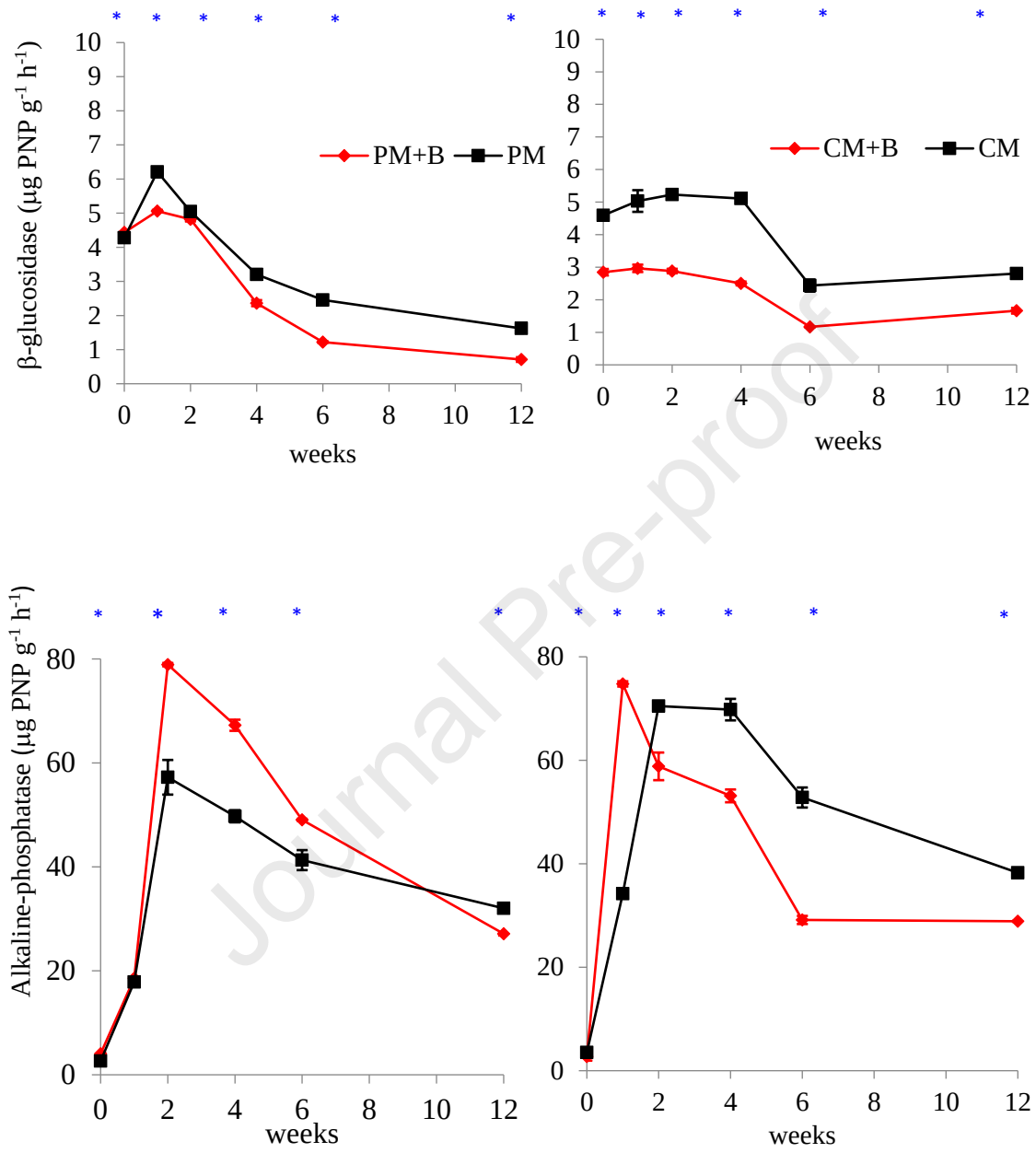

Fig 6. β-glucosidase activity and alkaline phosphatase activity and in composting sampled from poultry manure (PM) and cow manure (CM) treated with biochar (PM+B and CM+B). The figure shows the mean value (n = 3), with error bars indicating the standard deviation of the samples. Asterisk mark represents the significant difference. *p<0.05.

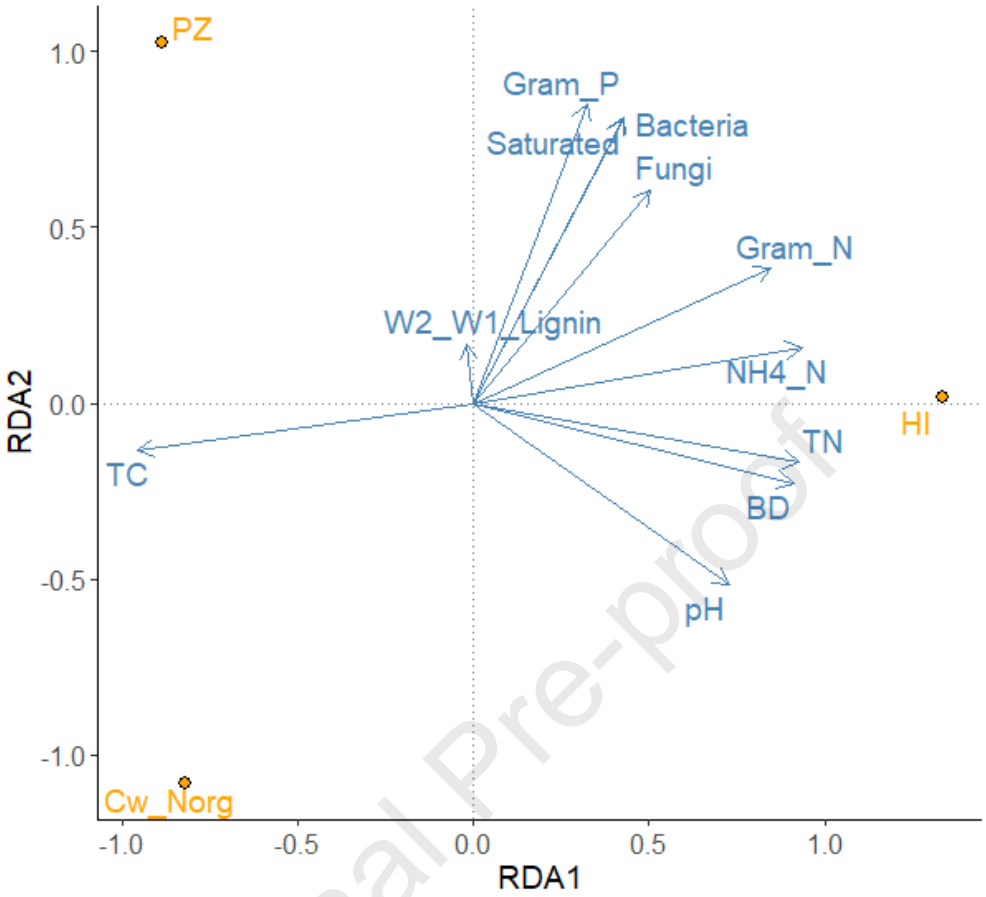

Fig. 7. Biplot of redundancy analysis (RDA) using various indicators of organic matter and key monitoring parameters at thermal stage of composting prepared from cattle manure (CM) and poultry manure (PM), with and without biochar. Data obtained from this study and from our previous our studies (Jindo et al 2012 & 2016). The list of the variables and its abbreviations are described in the supplemental material. The variables with orange letters are response variables (CH_4, CO_2, *pmoA*, *mcrA*).

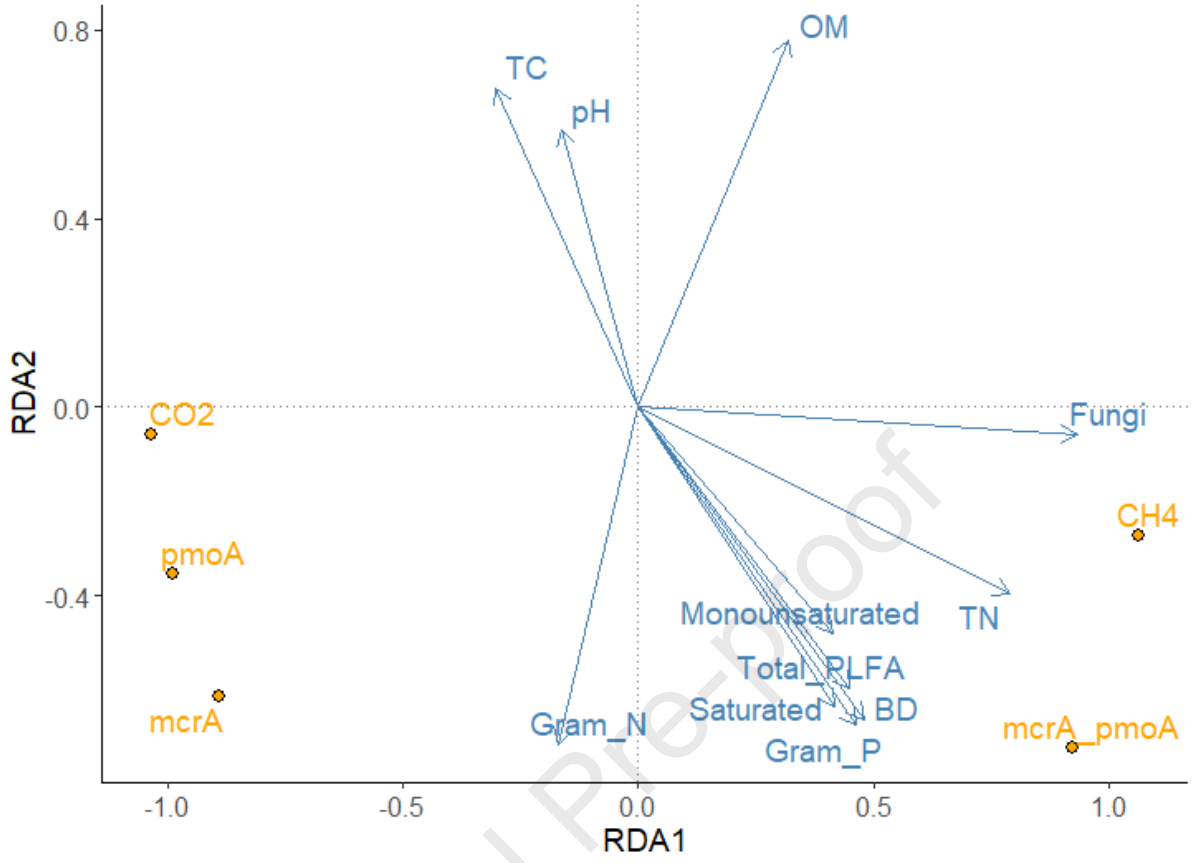

Fig, 8 Biplot of redundancy analysis (RDA) using various indicators of organic matter and key monitoring parameters at final stage of composting prepared from cattle manure (CM) and poultry manure (PM), with and without biochar. Data obtained from this study and from our previous our studies (Jindo et al 2012 & 2016; Sonoki et al., 2013). The list of the variables and its abbreviations are described in the supplemental material. The variables with orange letters are response variables (Cw_Norg: Total dissolved carbon/organic nitrogen; PZ: Polymerization (humic acid/fulvic acid); HI: Humification index).

Reference

Bekier, J., Drozd, J., Jamroz, E., Jarosz, B., Kocowicz, A., Walenczak, K., Weber, J., 2014. Changes in selected hydrophobic components during composting of municipal solid wastes. J Soils Sediments 14, 305–311. https://doi.org/10.1007/s11368-013-0696-0

Canellas, L.P., Dobbss, L.B., Oliveira, A.L., Chagas, J.G., Aguiar, N.O., Rumjanek, V.M., Novotny, E.H., Olivares, F.L., Spaccini, R., Piccolo, A., 2012. Chemical properties of humic matter as related to induction of plant lateral roots. Eur J Soil Sci 63, 315–324. https://doi.org/10.1111/j.1365-2389.2012.01439.x

Cao, X., Williams, P.N., Zhan, Y., Coughlin, S.A., McGrath, J.W., Chin, J.P., Xu, Y., 2023. Municipal solid waste compost: Global trends and biogeochemical cycling. Soil and Environmental Health. https://doi.org/10.1016/j.seh.2023.100038

Chandna, P., Nain, L., Singh, S., Kuhad, R.C., 2013. Assessment of bacterial diversity during composting of agricultural byproducts. BMC microbiology, 13, 99. https://doi.org/10.1186/1471-2180-13-99

Chen, W., Liao, X., Wu, Yinbao, Liang, J.B., Mi, J., Huang, J., Zhang, H., Wu, Yu, Qiao, Z., Li, X., Wang, Y., 2017. Effects of different types of biochar on methane and ammonia mitigation during layer manure composting. Waste Management 61, 506–515. https://doi.org/10.1016/J.WASMAN.2017.01.014

Duan, Y., Awasthi, M.K., Wu, H., Yang, J., Li, Z., Ni, X., Zhang, J., Zhang, Z., Li, H., 2022. Biochar regulates bacterial-fungal diversity and associated enzymatic activity during sheep manure composting. Bioresour Technol 346, 126647. https://doi.org/10.1016/J.BIORTECH.2021.126647

Eivazi, F., Tabatabai, M.A., 1988. Glucosidases and galactosidases in soils. Soil Biol Biochem 20, 601–606. https://doi.org/10.1016/0038-0717(88)90141-1

El Fels, L., Naylo, A., Jemo, M., Zrikam, N., Boularbah, A., Ouhdouch, Y., Hafidi, M., 2024. Microbial enzymatic indices for predicting composting quality of recalcitrant lignocellulosic substrates. Front Microbiol 15. https://doi.org/10.3389/fmicb.2024.1423728

Fang, C., Su, Y., Liang, Y., Han, L., He, X., Huang, G., 2022. Exploring the microbial mechanism of reducing methanogenesis during dairy manure membrane-covered aerobic composting at industrial scale. Bioresour Technol 354. https://doi.org/10.1016/j.biortech.2022.127214

Fracchia, L., Dohrmann, A.B., Martinotti, M.G., Tebbe, C.C., 2006. Bacterial diversity in a finished compost and vermicompost: Differences revealed by cultivation-independent analyses of PCR-amplified 16S rRNA genes. Appl Microbiol Biotechnol 71, 942–952. https://doi.org/10.1007/s00253-005-0228-y

Gu, S., Ji, Z., Li, X., Qin, H., Li, M., Zhang, L., Zhang, J., Huang, H., Luo, L., 2025. Organic matter components rather than microbial enzymes and genes predominate CO2/CH4 emissions during composting amended with biochar at different stages. Environmental Pollution 373. https://doi.org/10.1016/j.envpol.2025.126129

Guo, H., Gu, J., Wang, X., Song, Z., Yu, J., Lei, L., 2021. Microbial mechanisms related to the effects of bamboo charcoal and bamboo vinegar on the degradation of organic matter and methane emissions during composting. Environmental Pollution 272. https://doi.org/10.1016/j.envpol.2020.116013

Hagemann, N., Subdiaga, E., Orsetti, S., de la Rosa, J.M., Knicker, H., Schmidt, H.P., Kappler, A., Behrens, S., 2018. Effect of biochar amendment on compost organic matter composition following aerobic compositing of manure. Science of the Total Environment 613–614, 20–29. https://doi.org/10.1016/j.scitotenv.2017.08.161

Horiuchi, J.I., Ebie, K., Tada, K., Kobayashi, M., Kanno, T., 2003. Simplified method for estimation of microbial activity in compost by ATP analysis. Bioresour Technol 86, 95–98. https://doi.org/10.1016/S0960-8524(02)00108-6

Ji, Y., Cao, Y., Wang, Y., Wang, C., Qin, Z., Cai, W., Yang, Y., Yan, S., Guo, X., 2023. Effects of adding lignocellulose-degrading microbial agents and biochar on nitrogen metabolism and microbial community succession during pig manure composting. Environ Res 239, 117400. https://doi.org/10.1016/J.ENVRES.2023.117400

Jindo, K., Matsumoto, K., García Izquierdo, C., Sonoki, T., Sanchez-Monedero, M.A., 2014. Methodological interference of biochar in the determination of extracellular enzyme activities in composting samples. Solid Earth 5, 713–719. https://doi.org/10.5194/se-5-713-2014

Jindo, Keiji, Matsumoto, K., Sonoki, T., Bastida, F., García, C., Sánchez-Monedero, M.A., Hernández, T., Furukawa, T., 2012. Biochar influences the microbial community structure during manure composting with agricultural wastes. Science of The Total Environment 416, 476–481. https://doi.org/10.1016/j.scitotenv.2011.12.009

Jindo, K., Sonoki, T., Matsumoto, K., Canellas, L., Roig, A., Sanchez-Monedero, M.A., 2016. Influence of biochar addition on the humic substances of composting manures. Waste Management 49. https://doi.org/10.1016/j.wasman.2016.01.007

Jyoti K C, Reddy, K.R., Grubb, D.G.,, Green, S.J., 2022. Biogeochemical versus Conventional Landfill Soil Covers: Analysis of Gas Flow Profiles, Microbial Communities, and Mineralogy. J.Hazard.Toxic.Radioact. https://doi.org/10.1061/(ASCE)HZ.2153-5515.0000708

Khan, N., Bolan, N., Jospeh, S., Anh, M.T.L., Meier, S., Kookana, R., Borchard, N., Sánchez-Monedero, M.A., Jindo, K., Solaiman, Z.M., Alrajhi, A.A., Sarkar, B., Basak, B.B., Wang, H., Wong, J.W.C., Manu, M.K., Kader, M.A., Wang, Q., Li, R., Ok, Y.S., Withana, P.A., Qiu, R., 2023. Complementing compost with biochar for agriculture, soil remediation and climate mitigation, in: Advances in Agronomy. Academic Press Inc., pp. 1–90. https://doi.org/10.1016/bs.agron.2023.01.001

Li, J., Xie, T., Zhu, H., Zhou, J., Li, C., Xiong, W., Xu, L., Wu, Y., He, Z., Li, X., 2021. Alkaline phosphatase activity mediates soil organic phosphorus mineralization in a subalpine forest ecosystem. Geoderma 404, 115376. https://doi.org/10.1016/J.GEODERMA.2021.115376

Liu, Q., Chen, Z., Lin, Q., Yuan, J., Liu, Y., Huang, L., Feng, Y., 2024. Biochar compost associations affect the absorption, translocation and bioavailability of legacy and newly introduced cadmium in lettuce. J Clean Prod 451. https://doi.org/10.1016/j.jclepro.2024.142106

Ma, J., Ma, N.L., Fei, S., Liu, G., Wang, Y., Su, Y., Wang, X., Wang, J., Xie, Z., Chen, G., Sun, Y., Sun, C., 2024. Enhanced humification via lignocellulosic pretreatment in remediation of agricultural solid waste. Environmental Pollution 346, 123646. https://doi.org/10.1016/J.ENVPOL.2024.123646

Nguyen, B.T., Lehmann, J., Hockaday, W.C., Joseph, S., Masiello, C.A., 2010. Temperature sensitivity of black carbon decomposition and oxidation. Environ Sci Technol 44, 3324–3331. https://doi.org/10.1021/es903016y

Nikaeen, M., Nafez, A.H., Bina, B., Nabavi, B.B.F., Hassanzadeh, A., 2015. Respiration and enzymatic activities as indicators of stabilization of sewage sludge composting. Waste Management 39, 104–110. https://doi.org/10.1016/J.WASMAN.2015.01.028

Oviedo-Ocaña, E.R., Soto-Paz, J., Parra-Orobio, B.A., Zafra, G., Maeda, T., Galezo-Suárez, A.C., Diaz-Larotta, J.T., Sanchez-Torres, V., 2025. Effect of Biochar Addition in Two Different Phases of the Co-Composting of Green Waste and Food Waste: An Analysis of the Process, Product Quality and Microbial Community. Waste Biomass Valorization. https://doi.org/10.1007/s12649-024-02878-6

Palanivell, P., Susilawati, K., Ahmed, O.H., Majid, N.M., 2013. Compost and crude humic substances produced from selected wastes and their effects on zea mays l. nutrient uptake and growth. The Scientific World Journal 2013. https://doi.org/10.1155/2013/276235

Paredes, C., Roig, A., Bernal, M.P., Sánchez-Monedero, M.A., Cegarra, J., 2000. Evolution of organic matter and nitrogen during co-composting of olive mill wastewater with solid organic wastes, Biol Fertil Soils. 32, 222–227. https://doi.org/10.1007/s003740000239

Piotrowska-Długosz, A., Długosz, J., Frąc, M., Gryta, A., Breza-Boruta, B., 2022. Enzymatic activity and functional diversity of soil microorganisms along the soil profile – A matter of soil depth and soil-forming processes. Geoderma 416, 115779. https://doi.org/10.1016/J.GEODERMA.2022.115779

Pivato, A., Malesani, R., Bocchi, S., Rafieenia, R., Schievano, A., 2023. Biochar addition to compost heat recovery systems improves heat conversion yields. Front Energy Res 11. https://doi.org/10.3389/fenrg.2023.1327136

Sanchez-Monedero, M.A., Cayuela, M.L., Roig, A., Jindo, K., Mondini, C., Bolan, N., 2018. Role of biochar as an additive in organic waste composting. Bioresour Technol 247. https://doi.org/10.1016/j.biortech.2017.09.193

Shi, Z., Xu, G., Deng, J., Dong, M., Murugadoss, V., Liu, C., Shao, Q., Wu, S., Guo, Z., 2019. Structural characterization of lignin from D. sinicus by FTIR and NMR techniques. Green Chem Lett Rev. https://doi.org/10.1080/17518253.2019.1627428

Sonoki, T., Furukawa, T., Jindo, K., Suto, K., Aoyama, M., Sánchez-Monedero, M.A., 2013. Influence of biochar addition on methane metabolism during thermophilic phase of composting. J Basic Microbiol 53. https://doi.org/10.1002/jobm.201200096

Spaccini, R., Piccolo, A., 2009. Molecular characteristics of humic acids extracted from compost at increasing maturity stages. Soil Biol Biochem 41, 1164–1172. https://doi.org/10.1016/j.soilbio.2009.02.026

Spaccini, R., Piccolo, A., Conte, P., Haberhauer, G., Gerzabek, M.H., 2002. Increased soil organic carbon sequestration through hydrophobic protection by humic substances. Soil Biol Biochem 34, 1839–1851. https://doi.org/10.1016/S0038-0717(02)00197-9

Swarnam, T.P., Velmurugan, A., Pandey, S.K., Dam Roy, S., 2016. Enhancing nutrient recovery and compost maturity of coconut husk by vermicomposting technology. Bioresour Technol 207, 76–84. https://doi.org/10.1016/j.biortech.2016.01.046

Toundou, O., Pallier, V., Feuillade-Cathalifaud, G., Tozo, K., 2021. Impact of agronomic and organic characteristics of waste composts from Togo on Zea mays L. nutrients contents under water stress. J Environ Manage 285, 112158. https://doi.org/10.1016/J.JENVMAN.2021.112158

Wang, C., Tu, Q., Dong, D., Strong, P.J., Wang, H., Sun, B., Wu, W., 2014. Spectroscopic evidence for biochar amendment promoting humic acid synthesis and intensifying humification during composting. J Hazard Mater 280, 409–416. https://doi.org/10.1016/J.JHAZMAT.2014.08.030

Wang, H., Shao, T., Zhou, Y., Long, X., Rengel, Z., 2023. The effect of biochar prepared at different pyrolysis temperatures on microbially driven conversion and retention of nitrogen during composting. Heliyon 9. https://doi.org/10.1016/j.heliyon.2023.e13698

Wang, J., Xiong, Z., Kuzyakov, Y., 2016. Biochar stability in soil: Meta-analysis of decomposition and priming effects. GCB Bioenergy. https://doi.org/10.1111/gcbb.12266

Wang, S., Meng, Q., Zhu, Q., Niu, Q., Yan, H., Li, K., Li, G., Li, X., Liu, H., Liu, Y., Li, Q., 2021. Efficient decomposition of lignocellulose and improved composting performances driven by thermally activated persulfate based on metagenomics analysis. Science of the Total Environment 794. https://doi.org/10.1016/j.scitotenv.2021.148530

Wei, Q., Zhang, J., Luo, F., Shi, D., Liu, Y., Liu, S., Zhang, Q., Sun, W., Yuan, J., Fan, H., Wang, H., Qi, L., Liu, G., 2022. Molecular mechanisms through which different carbon sources affect denitrification by Thauera linaloolentis: Electron generation, transfer, and competition. Environ Int 170, 107598. https://doi.org/10.1016/J.ENVINT.2022.107598

Xiao, R., Awasthi, M.K., Li, R., Park, J., Pensky, S.M., Wang, Q., Wang, J.J., Zhang, Z., 2017. Recent developments in biochar utilization as an additive in organic solid waste composting: A review. Bioresour Technol 246, 203–213. https://doi.org/10.1016/J.BIORTECH.2017.07.090

Xin, P., Zhang, Y., Jiang, N., Chen, Z., Chen, L., 2024. Neutral soil pH conditions favor the inhibition of phenol on hydrolase activities and soil organic carbon mineralization. Eur J Soil Biol 121, 103621. https://doi.org/10.1016/J.EJSOBI.2024.103621

Yu, H., Xie, B., Khan, R., Shen, G., 2019. The changes in carbon, nitrogen components and humic substances during organic-inorganic aerobic co-composting. Bioresour Technol 271, 228–235. https://doi.org/10.1016/j.biortech.2018.09.088

Yu, J., Gu, J., Wang, X., Lei, L., Guo, H., Song, Z., Sun, W., 2023. Exploring the mechanism associated with methane emissions during composting: Inoculation with lignocellulose-degrading microorganisms. J Environ Manage 325. https://doi.org/10.1016/j.jenvman.2022.116421

Yuan, Y., Chen, H., Yuan, W., Williams, D., Walker, J.T., Shi, W., 2017. Is biochar-manure co-compost a better solution for soil health improvement and N2O emissions mitigation? Soil Biol Biochem 113, 14–25. https://doi.org/10.1016/j.soilbio.2017.05.025

Zainudin, M.H., Mustapha, N.A., Maeda, T., Ramli, N., Sakai, K., Hassan, M., 2020. Biochar enhanced the nitrifying and denitrifying bacterial communities during the composting of poultry manure and rice straw. Waste Management 106, 240–249. https://doi.org/10.1016/J.WASMAN.2020.03.029

Zhai, S., Wang, K., Yu, F., Gao, Z., Yang, X., Cao, X., Shaghaleh, H., Hamoud, Y.A., 2025. Effects of Trichoderma harzianum combined with Phanerochaete chrysosporium on lignin degradation and humification during chicken manure and rice husk composting. Front Microbiol 16. https://doi.org/10.3389/fmicb.2025.1515931

Title: Stabilizing organic matter and reducing methane emissions in composting with biochar to strengthen the role of compost in soil health.

Authors: Keiji Jindo[a]*, Tomonori Sonoki[b], Miguel A. Sánchez-Monedero[c],

[a]Agrosystems Research, Wageningen University & Research, P.O. Box 16, 6700 AA, Wageningen, the Netherlands. keiji.jindo@wur.nl

[b]Faculty of Agriculture and Life Science, Hirosaki University, Hirosaki, Aomori, 036-8561, Japan. sonoki@hirosaki-u.ac.jp.

[c]Department of Soil and Water Conservation and Organic Waste Management, CEBAS-CSIC, Campus Universitario de Espinardo, Murcia, Spain. monedero@cebas.csic.es

*Corresponding author: Keiji Jindo (keiji.jindo@wur.nl)

Tel.: + 31 639072812

Declaration of Interest statement

The authors declare that they have no conflict of interest.